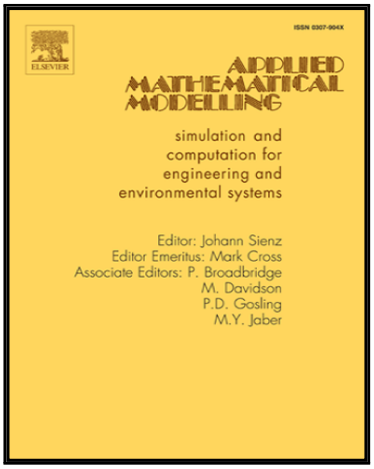

A threshold policy to interrupt transmission of West Nile Virus to birds

Weike Zhou, Yanni Xiao, Robert A. Cheke

PII: S0307-904X(16)30299-2
DOI: 10.1016/j.apm.2016.05.040
Reference: APM 11193

To appear in: *Applied Mathematical Modelling*

Received date: 22 November 2015
Revised date: 11 May 2016
Accepted date: 18 May 2016

Please cite this article as: Weike Zhou, Yanni Xiao, Robert A. Cheke, A threshold policy to interrupt transmission of West Nile Virus to birds, *Applied Mathematical Modelling* (2016), doi: 10.1016/j.apm.2016.05.040

Highlights

- Propose a Filippov model of West Nile Virus with density-dependent culling strategy.
- Solutions approach either endemic equilibrium for subsystems or a pseudo-equilibrium.
- Results indicate that a previously chosen level of infected birds can be maintained.
- Strengthening mosquito culling is beneficial to curbing the spread of WNV.

A threshold policy to interrupt transmission of West Nile Virus to birds

Weike Zhou[a], Yanni Xiao[a]*, Robert A. Cheke[b]

[a] *Department of Applied Mathematics, School of Mathematics and Statistics, Xi'an Jiaotong University, Xi'an 710049, PR China*
[b] *Natural Resources Institute, University of Greenwich at Medway, Central Avenue, Chatham Maritime, Chatham, Kent, ME4 4TB, UK*

Abstract

This paper proposes a model of West Nile Virus (WNV) with a Filippov-type control strategy of culling mosquitoes implemented once the number of infected birds exceeds a threshold level. The long-term dynamical behaviour of the proposed non-smooth system is investigated. It is shown that as the threshold value varies, model solutions ultimately approach either one of two endemic equilibria for two subsystems or a pseudo-equilibrium on the switching surface, which is a novel steady state. The results indicate that a previously chosen level of infected birds can be maintained when the threshold policy and other parameters are chosen properly. Numerical studies show that under the threshold policy, strengthening mosquito culling together with protecting bird population is beneficial to curbing the spread of WNV.

Keywords: WNV, Filippov model, Threshold policy, Global dynamics

1. Introduction

West Nile Virus (WNV), which was first identified in the West Nile subregion of Uganda in 1937, is a mosquito-borne single-stranded RNA virus belonging to the genus Flavivirus in the family Flaviviridae [1–4]. WNV is transmitted between the vector mosquitoes and birds, humans, horses, dogs and other animals, with birds being the most commonly infected animals as well as the principal reservoir hosts [5, 6]. Humans and other animals can be infected by the bite of an infectious mosquito that has fed from the blood of an infected bird, but they do not transmit the disease. Thus, WNV is maintained in a mosquito-bird-human transmission cycle in nature [7, 12]. WNV has now spread globally and rapidly. The first case in North America was reported in 1999, followed by nearly 40,000 cases and 1554 deaths reported in 52 states up to 2013 [8, 9], causing a great deal of concern among the public as well as within federal and State public health and natural resource management agencies.

Owing to the absence of both effective anti-WNV therapeutic treatment for and a vaccine against WNV, it is essential to develop preventive measures or culling strategies to attempt to halt the spread of WNV. It is well known that culling as a tool to control the spread of vector-borne diseases has been extensively used in many studies. For example, in [10], Gourley et al. showed that culling is an effective strategy to control the spread of vector-borne diseases such as WNV and the disease can be eradicated by culling the vector. Tchuenche et al. [11] also investigated the effectiveness of culling strategies on the control of monkeypox transmission while the results indicated that the culling of animals may have counter-productive consequences of increasing cases in children. Numerous mathematical models [4–6, 12–17] for WNV with cross-infection between mosquitoes and birds have been formulated based on Ross-Macdonald equations [18, 19], aiming to predict disease dynamics and evaluate possible control strategies. Thomas and Urena [12] formulated a differential equation model to investigate the efficacy of pesticide spraying to reduce mosquito populations and determine how many mosquitoes needed to be killed to ensure elimination of the virus. In [13], a non-spatial SIR model was formulated to examine the emerging WNV epidemic in North America. Bowman et al.

*Corresponding author. Tel:+86 29 82663156, Fax:+86 29 82668551
Email address: yxiao@mail.xjtu.edu.cn (Yanni Xiao[a])

[4], proposed a single-season differential equation model in a mosquito-bird-human community (an isolated patch) to assess preventive strategies against WNV. Lewis et al. [17] extended the models formulated in [12, 13] by including impulsive events and concluded that a reduction in bird density would exacerbate the epidemic with model in [13], while it would help to maintain the epidemic on the basis of the model in [12]. Blayneh et al. [6] slightly modified the model in [4] to assess the impact of some anti-WNV control measures and obtained the threshold conditions for WNV outbreaks and demonstrated the existence of backward bifurcation in their model. Jiang et al. [16] showed that the dynamics of the whole model in [4] were indeed determined by the four dimensional system involving only the mosquitoes and birds, and suggested that the most effective and realistic strategy to prevent the spread of WNV was to control the mosquitoes. Further, considering impulsive mosquito culling, Hu and Liu et al. [20] formulated a compartmental model in the form of a non-autonomous system of delay differential equations with culling impulses at specific times based on impulsive models [10, 21]. Xu et al. [22] formulated two impulsive models considering periodic or state-dependent pesticide sprays as control measures to investigate the transmission of WNV between mosquitoes and birds.

In the continuous models and the models with impulsive control measures at some fixed moments [10, 12–17, 20–22], control is always applied regardless of the population size of infected individuals, which may waste resources because it is not necessary to implement a control strategy when the population density of infected individuals is low. All such models assume, explicitly or implicitly, that interventions are implemented, irrespective of the case numbers and the timing of the implementations. However, differential equation models with state-dependent pulses are proposed to represent strategies that are implemented once the number of infected birds reaches threshold [22]. A common assumption in such models is that the human control activities occur instantaneously, but this is seldom the case with interventions or control strategies usually lasting for a given period. Recently, a threshold policy (TP) has been proposed to describe density-dependent and persistent interventions, which are implemented when the case numbers exceeds a certain value and are suspended when they fall below a critical level [23–29]. Therefore, our main purpose is to extend the existing models on WNV as a non-smooth system by considering density-dependent and non-instantaneous control measures, based on the threshold policy idea, to examine whether a threshold policy could be used to control the transmission dynamics of WNV more effectively than reliance on existing impulsive differential equations. We then aim to identify the most rational threshold or most effective strategies to control the transmission of WNV and keep the number of infected birds relatively low.

To achieve the above goals, we fomulate a non-smooth model with a Filippov-type control strategy by assuming that control interventions are implemented once the number of infected birds exceeds a certain level, investigate the transmission of WNV between mosquitoes and birds theoretically, and draw some interesting conclusions. The paper is organized as follows. In Section 2, an epidemic model with a Filippov-type control is proposed to describe the non-instantaneous control and the dynamics of two subsystems are analyzed. In Section 3, sliding mode dynamics and the existence of the pseudo-equilibrium are investigated. The boundary node bifurcation is discussed in Section 4 and the global behaviour of the system is described in Section 5. Finally, we provide biological conclusions and discussion in Section 6.

2. Epidemic model of WNV transmission with a Filippov-type control and preliminaries

Under threshold policy (TP), control is implemented when the case number exceeds a critical level, while it is suppressed when it is below the specific threshold level. We assume that mosquitoes and birds are culled when the number of infected birds in a population exceeds a certain level E_{I_b}. Let $N_m(t)$ represent the total female mosquito population at time t, divided into two classes: uninfected susceptible female mosquitoes ($S_m(t)$) and female mosquitoes infected with WNV ($I_m(t)$) (i.e. $N_m(t) = S_m(t) + I_m(t)$). Similarly, for the birds, $N_b(t)$ denotes the total bird population at time t and $N_b(t) = S_b(t) + I_b(t)$ in which $S_b(t)$ is the number of susceptible birds and $I_b(t)$ stands for birds infected with WNV. The recruitment rate and natural death rate are Λ and μ, for which we use the subscript m and b to identify

Table 1: Definitions of variables and parameters in the model

Variables	Description		
$N_m(t)$	Total population of female mosquitoes		
$S_m(t)$	Susceptible population of female mosquitoes		
$I_m(t)$	Infected population of female mosquitoes		
$N_b(t)$	Total population of birds		
$S_b(t)$	Susceptible population of birds		
$I_b(t)$	Infected population of birds		
Parameters	Description	Value	Resource
Λ_m	Recruitment rate of mosquitoes (per day)	5	Assumed
Λ_b	Recruitment rate of birds (per day)	2	[22]
c	Average biting rate of the mosquitoes (per day)		Varies
β_{mb}	Transmission probability from birds to mosquitoes	0.3	[5]
β_{bm}	Transmission probability from mosquitoes to birds	0.18	Assumed
μ_m	Natural death rate of mosquitoes (per day)	2	Assumed
μ_b	Natural death rate of birds (per day)	0.8	Assumed
f_m	Culling rate of mosquitoes (per day)		Varies
f_b	Culling rate of birds (per day)		Varies
E_{I_b}	Critical level of birds		Varies
ε	Whether the culling strategy is implemented	0 or 1	[23]

the female mosquitoes and birds. The susceptible mosquitoes enter into the infected mosquitoes category when they bite infected birds, at an average biting rate c and with a probability β_{mb} for transmission of WNV from birds to mosquitoes. Similarly, susceptible birds join the infected birds class when they are bitten by infected mosquitoes at an average biting rate c and with a probability β_{bm} of transmission of WNV from mosquitoes to birds. f_m and f_b denote the culling rates of mosquitoes and birds, respectively. The model variables and definitions of the parameters are listed in Table 1.

$$\begin{cases} \frac{dS_m}{dt} = \Lambda_m - c\beta_{mb}\frac{I_b}{N_b}S_m - \mu_m S_m - \varepsilon f_m S_m, \\ \frac{dI_m}{dt} = c\beta_{mb}\frac{I_b}{N_b}S_m - \mu_m I_m - \varepsilon f_m I_m, \\ \frac{dS_b}{dt} = \Lambda_b - c\beta_{bm}\frac{S_b}{N_b}I_m - \mu_b S_b - \varepsilon f_b S_b, \\ \frac{dI_b}{dt} = c\beta_{bm}\frac{S_b}{N_b}I_m - \mu_b I_b - \varepsilon f_b I_b, \end{cases} \tag{1}$$

with

$$\varepsilon = \begin{cases} 0, & H(I_m,\, I_b) < 0, \\ 1, & H(I_m,\, I_b) > 0, \end{cases} \tag{2}$$

where $H(I_m,\, I_b) = I_b - E_{I_b}$ is the threshold function. Note that $\varepsilon = 0$ means the absence of culling while $\varepsilon = 1$ indicates that culling occurs.

Regarding ε as a parameter, we know that the populations of mosquitoes and birds, N_m, N_b, follow

$$N_m(\varepsilon) \to \frac{\Lambda_m}{\mu_m + \varepsilon f_m}, \quad N_b(\varepsilon) \to \frac{\Lambda_b}{\mu_b + \varepsilon f_b},$$

as $t \to +\infty$. Then, substituting $N_m(\varepsilon),\ N_b(\varepsilon)$ and $S_m = N_m(\varepsilon) - I_m,\ S_b = N_b(\varepsilon) - I_b$ into the second and fourth equations of system (1), we have the following non-smooth dynamic system

$$\begin{cases} \frac{dI_m}{dt} = c\beta_{mb}\frac{(\mu_b+\varepsilon f_b)I_b}{\Lambda_b}\left(\frac{\Lambda_m}{\mu_m+\varepsilon f_m} - I_m\right) - (\mu_m + \varepsilon f_m)I_m, \\ \frac{dI_b}{dt} = c\beta_{bm}\left(1 - \frac{(\mu_b+\varepsilon f_b)I_b}{\Lambda_b}\right)I_m - (\mu_b + \varepsilon f_b)I_b. \end{cases} \tag{3}$$

Denote $X = (I_m, I_b)^T$, and define the hyperplane

$$\Sigma := \{X \in R_+^2 \mid H(X) = 0\},$$

separating R_+^2 into two regions:

$$\Omega_1 := \{X \in R_+^2 \mid H(X) < 0\}, \ \ \Omega_2 := \{X \in R_+^2 \mid H(X) > 0\}.$$

Denote the right-hand sides of (3) in region Ω_i by $F_i(X)$, and denote the components of $F_i(X)$ by F_{i1}, F_{i2} for $i = 1,2$, respectively. Then

$$F_1(X) = \begin{pmatrix} F_{11} \\ F_{12} \end{pmatrix} = \begin{pmatrix} c\beta_{mb}\frac{\mu_b I_b}{\Lambda_b}(\frac{\Lambda_m}{\mu_m} - I_m) - \mu_m I_m \\ c\beta_{bm}(1 - \frac{\mu_b I_b}{\Lambda_b})I_m - \mu_b I_b \end{pmatrix},$$

$$F_2(X) = \begin{pmatrix} F_{21} \\ F_{22} \end{pmatrix} = \begin{pmatrix} c\beta_{mb}\frac{(\mu_b+f_b) I_b}{\Lambda_b}(\frac{\Lambda_m}{\mu_m+f_m} - I_m) - (\mu_m+f_m) I_m \\ c\beta_{bm}(1 - \frac{(\mu_b+f_b) I_b}{\Lambda_b})I_m - (\mu_b+f_b) I_b \end{pmatrix}.$$

Thus the system (3) with (2) can be rewritten as the following Filippov system:

$$\dot{X} = \begin{cases} F_1(X), \ \ X \in \Omega_1, \\ F_2(X), \ \ X \in \Omega_2. \end{cases} \tag{4}$$

The main characteristic of a Filippov system is that there is no action taken when the value of the threshold function is below a previously chosen threshold level; otherwise control is applied, resulting in a variable structure system with two distinct structures: a $free-system$ and a $control-system$. In the following, we call system (4) defined in Ω_1 as system S^1 (i.e. system (5) in the following section) and defined in Ω_2 as system S^2 (i.e. system (9) in the following section).

2.1. Analysis for system S^1

When $I_b < E_{I_b}$, resulting in $\varepsilon = 0$, culling is not implemented and system (4) becomes the following system (5), called the $free-system$.

$$\begin{cases} \frac{dI_m}{dt} = c\beta_{mb}\frac{\mu_b I_b}{\Lambda_b}(\frac{\Lambda_m}{\mu_m} - I_m) - \mu_m I_m, \\ \frac{dI_b}{dt} = c\beta_{bm}(1 - \frac{\mu_b I_b}{\Lambda_b})I_m - \mu_b I_b. \end{cases} \tag{5}$$

It is easy to show that the basic reproduction number for system (5) is $R_{01} = \frac{c^2\beta_{bm}\beta_{mb}\Lambda_m}{\mu_m^2\Lambda_b}$. The disease-free equilibrium (DFE) $E_{01}(0,0)$ is feasible all the time, and the corresponding characteristic equation is

$$\lambda^2 + (\mu_m + \mu_b)\lambda + \mu_m\mu_b - c^2\beta_{mb}\beta_{bm}\frac{\mu_b\Lambda_m}{\mu_m\Lambda_b} = 0, \tag{6}$$

which has two negative roots for $R_{01} < 1$ and one positive root and one negative root for $R_{01} > 1$. Hence DFE E_{01} is locally asymptotically stable for $R_{01} < 1$ and unstable for $R_{01} > 1$. When $R_{01} > 1$, there exists a positive equilibrium $E_1(I_{m1}^*, I_{b1}^*)$, where

$$I_{b1}^* = \frac{c^2\beta_{bm}\beta_{mb}\frac{\Lambda_m}{\mu_m} - \mu_m\Lambda_b}{c^2\beta_{bm}\beta_{mb}\frac{\Lambda_m}{\mu_m}\frac{\mu_b}{\Lambda_b} + c\beta_{mb}\mu_b} = \frac{\Lambda_b}{\mu_b}\frac{R_{01}-1}{R_{01}+\frac{c\beta_{mb}}{\mu_m}}, \quad I_{m1}^* = \frac{\mu_b I_{b1}^*}{c\beta_{bm}(1-\frac{\mu_b I_{b1}^*}{\Lambda_b})}.$$

Based on the Jacobian matrix of (5) at E_1, we get the corresponding characteristic equation

$$\lambda^2 + \bar{A}\lambda + \bar{B} = 0, \tag{7}$$

where

$$\begin{aligned}\bar{A} &= \mu_m + c\beta_{mb}\tfrac{\mu_b}{\Lambda_b}I^*_{b1} + \mu_b + c\beta_{bm}\tfrac{\mu_b}{\Lambda_b}I^*_{m1} > 0,\\ \bar{B} &= (\mu_m + c\beta_{mb}\tfrac{\mu_b}{\Lambda_b}I^*_{b1})(\mu_b + c\beta_{bm}\tfrac{\mu_b}{\Lambda_b}I^*_{m1}) - c^2\beta_{mb}\beta_{bm}\tfrac{\mu_b}{\Lambda_b}(\tfrac{\Lambda_m}{\mu_m} - I^*_{m1})(1 - \tfrac{\mu_b}{\Lambda_b}I^*_{b1})\\ &= (\mu_m + c\beta_{mb}\tfrac{\mu_b}{\Lambda_b}I^*_{b1})(\mu_b + c\beta_{bm}\tfrac{\mu_b}{\Lambda_b}I^*_{m1}) - \mu_m\mu_b\\ &> 0.\end{aligned}$$

Note that

$$\begin{aligned}\Delta_1 &= \bar{A}^2 - 4\bar{B}\\ &= (\mu_m + c\beta_{mb}\tfrac{\mu_b}{\Lambda_b}I^*_{b1} + \mu_b + c\beta_{bm}\tfrac{\mu_b}{\Lambda_b}I^*_{m1})^2 - 4[(\mu_m + c\beta_{mb}\tfrac{\mu_b}{\Lambda_b}I^*_{b1})(\mu_b + c\beta_{bm}\tfrac{\mu_b}{\Lambda_b}I^*_{m1}) - \mu_m\mu_b]\\ &= [(\mu_m + c\beta_{mb}\tfrac{\mu_b}{\Lambda_b}I^*_{b1}) - (\mu_b + c\beta_{bm}\tfrac{\mu_b}{\Lambda_b}I^*_{m1})]^2 + 4\mu_m\mu_b\\ &> 0,\end{aligned}$$

indicating that the above eigenfunction has two negative roots. Thus the positive equilibrium E_1 is a stable node when $R_{01} > 1$. Letting the Dulac function [30] be $\mathscr{B} = \frac{1}{I_m I_b}$, we have

$$\frac{\partial(\mathscr{B}F_{11})}{\partial I_m} + \frac{\partial(\mathscr{B}F_{12})}{\partial I_b} = -[c\beta_{mb}\tfrac{\mu_b\Lambda_m}{\mu_m\Lambda_b}\tfrac{1}{I_m^2} + c\beta_{bm}\tfrac{1}{I_b^2}] < 0, \tag{8}$$

suggesting that there is no limit cycle of system (5). Therefore according to Bendixson-Dulac criterion [30], we have the following theorem.

Theorem 1. *When $R_{01} < 1$, the disease-free equilibrium of system (5) is globally asymptotically stable; when $R_{01} > 1$, E_{01} is unstable while the unique endemic equilibrium $E_1(I^*_{m1}, I^*_{b1})$ is feasible and is a globally asymptotically stable node.*

2.2. Analysis for system S^2

When $I_b > E_{I_b}$, suggesting $\varepsilon = 1$, then the culling intervention is carried out and model (4) becomes the following system (9), which we call the *control − system*.

$$\begin{cases}\frac{dI_m}{dt} = c\beta_{mb}\frac{(\mu_b+f_b)I_b}{\Lambda_b}(\frac{\Lambda_m}{\mu_m+f_m} - I_m) - (\mu_m + f_m)I_m,\\ \frac{dI_b}{dt} = c\beta_{bm}(1 - \frac{(\mu_b+f_b)I_b}{\Lambda_b})I_m - (\mu_b + f_b)I_b.\end{cases} \tag{9}$$

It is easy to show that the basic reproduction number of system (9) is $R_{02} = \frac{c^2\beta_{bm}\beta_{mb}\Lambda_m}{(\mu_m+f_m)^2\Lambda_b}$. Similarly as analysis for system S^1, the disease-free equilibrium $E_{02}(0,0)$ exists all the time and is locally asymptotically stable when $R_{02} < 1$; when $R_{02} > 1$, E_{02} is unstable and there exists a positive equilibrium $E_2(I^*_{m2}, I^*_{b2})$, which is an asymptotically stable node, where

$$I^*_{b2} = \frac{c^2\beta_{bm}\beta_{mb}\frac{\Lambda_m}{\mu_m+f_m} - (\mu_m+f_m)\Lambda_b}{c^2\beta_{bm}\beta_{mb}\frac{\Lambda_m}{\mu_m+f_m}\frac{\mu_b+f_b}{\Lambda_b} + c\beta_{mb}(\mu_b+f_b)} = \frac{\Lambda_b}{\mu_b+f_b}\frac{R_{02}-1}{R_{02} + \frac{c\beta_{mb}}{\mu_m+f_m}}, \quad I^*_{m2} = \frac{(\mu_b+f_b)I^*_{b2}}{c\beta_{bm}(1 - \frac{(\mu_b+f_b)I^*_{b2}}{\Lambda_b})}.$$

By using the same Dulac function $\mathscr{B} = \frac{1}{I_m I_b}$, we can show that there is no limit cycle of system (9) either. Therefore according to Bendixson-Dulac criterion [30], we have the following theorem.

Theorem 2. *When $R_{02} < 1$, the disease-free equilibrium of system (9) is globally asymptotically stable; when $R_{02} > 1$, E_{02} is unstable while the unique endemic equilibrium $E_2(I^*_{m2}, I^*_{b2})$ is feasible and is a globally asymptotically stable node.*

By simple calculation, we get: $R_{02} < R_{01}$, $I^*_{b2} < I^*_{b1}$, $I^*_{m2} < I^*_{m1}$. Note that the endemic equilibria of the two subsystems (i.e. $E_1(I^*_{m1}, I^*_{b1})$ and $E_2(I^*_{m2}, I^*_{b2})$) could be either in region Ω_1 or in Ω_2. If $E_1(E_2)$ is located in $\Omega_1(\Omega_2)$,

we have what we call the real equilibrium, denoted by $E_1^R(E_2^R)$, and if $E_1(E_2)$ is located in $\Omega_2(\Omega_1)$, we have the virtual equilibrium, denoted by $E_1^V(E_2^V)$. Regular equilibrium is a term applicable to both the real and virtual equilibria. In particular, when $E_{I_b} > I_{b1}^*$, E_1 is a real equilibrium denoted by E_1^R while E_2 is a virtual equilibrium denoted by E_2^V; when $I_{b2}^* < E_{I_b} < I_{b1}^*$, both E_1 and E_2 are virtual, denoted by E_1^V and E_2^V, respectively; and when $E_{I_b} < I_{b2}^*$, E_1 is a virtual equilibrium denoted by E_1^V while E_2 is a real equilibrium denoted by E_2^R . If $R_{01} < 1$, the two positive endemic equilibria E_1, E_2 for two subsystems do not exist, the disease is consequently eradicated, then the control strategy will not be considered further. Thus, in the following we only consider the case when $R_{01} > 1$.

3. Sliding mode and its dynamics

We initially examine the existence of the sliding mode. A 'sliding mode' exists if there are regions in the vicinity of manifold Σ where the vector fields of both structures of the system (4) are directed towards each other. Two basic methods, namely, the Filippov convex method [31] and Utkin's equivalent control method [32], were developed for a sliding mode to occur on the surface of a discontinuity. For system (4) with (2), let

$$\sigma(X) = \langle H_X(X), F_1(X)\rangle \langle H_X(X), F_2(X)\rangle, \tag{10}$$

where $\langle \cdot, \cdot \rangle$ denotes the standard scalar product. Then the sliding domain is defined as

$$\Sigma_S = \{X \in \Sigma : \sigma(X) \leq 0\}.$$

The positively invariant set of system (5) is $\mathfrak{D}_1 = \{(I_m, I_b) \in R_+^2 : 0 < I_m \leq \frac{\Lambda_m}{\mu_m}, 0 < I_b \leq \frac{\Lambda_b}{\mu_b}\}$, and the positively invariant set of system (9) is $\mathfrak{D}_2 = \{(I_m, I_b) \in R_+^2 : 0 < I_m \leq \frac{\Lambda_m}{\mu_m + f_m}, 0 < I_b \leq \frac{\Lambda_b}{\mu_b + f_b}\}$. Hence we only discuss the case of $0 < E_{I_b} < \frac{\Lambda_b}{\mu_b + f_b}$. It is easy to verify that the sliding mode exists since the following sliding domain where the two adjacent vector fields point towards the manifold is not empty:

$$\Sigma_S = \left\{ (I_m, I_b) | \frac{\mu_b E_{I_b}}{c\beta_{bm}(1 - \frac{\mu_b E_{I_b}}{\Lambda_b})} \leq I_m \leq \frac{(\mu_b + f_b) E_{I_b}}{c\beta_{bm}(1 - \frac{(\mu_b + f_b) E_{I_b}}{\Lambda_b})}, I_b = E_{I_b} \right\}.$$

Denote the two endpoints of Σ_S by $T_1(I_{m1}, E_{I_b})$ and $T_2(I_{m1}, E_{I_b})$, respectively, with

$$I_{m1} = \frac{\mu_b E_{I_b}}{c\beta_{bm}(1 - \frac{\mu_b E_{I_b}}{\Lambda_b})}, \quad I_{m2} = \frac{(\mu_b + f_b) E_{I_b}}{c\beta_{bm}(1 - \frac{(\mu_b + f_b) E_{I_b}}{\Lambda_b})}.$$

Then the coordinates of the two endpoints of Σ_S are $T_1(I_{m1}, E_{I_b})$, $T_2(I_{m2}, E_{I_b})$. $\overline{T_1 T_2}$ is called the sliding segment.

Note that the solutions of the system (4) can be constructed by concatenating standard solutions in Ω_1, Ω_2 and sliding solutions on the switching line Σ. Hence the dynamics can be determined by either vector field F_1 alone or F_2 alone, i.e. qualitative behaviour not involving structural changes in the sliding segment [33], or determined by both vector fields F_1, F_2 and sliding dynamics of the system (4), i.e. qualitative behaviour involving some structural changes in the sliding segment. Therefore, we need to determine the sliding mode dynamics or sliding solutions on Σ for the system (4) in order to investigate the system (4), which can be realized by employing the well-known Filippov convex method [31] or Utkin's equivalent control method [32]. Next, we will address the dynamics of system (4) on the sliding domain Σ_S by using a formal procedure, following the equivalent control method developed by Utkin [32]. By means of algebraic manipulations, we can eliminate ε. Let $\frac{dI_b}{dt} = c\beta_{bm}\frac{N_b(\varepsilon) - I_b}{N_b(\varepsilon)} I_m - \mu_b I_b - \varepsilon f_b I_b = 0$, solving with respect to ε, we have

$$\varepsilon = \frac{c\beta_{bm}I_m - \mu_b(c\beta_{bm}\frac{E_{I_b}}{\Lambda_b}I_m + E_{I_b})}{(c\beta_{bm}\frac{E_{I_b}}{\Lambda_b}I_m + E_{I_b})f_b}. \tag{11}$$

Substituting ε given above and $I_b = E_{I_b}$ into the first equation of (3) gives the differential equations of the sliding mode dynamics on the switching line:

$$\begin{aligned}\frac{dI_m}{dt} = & -\frac{c^2\beta_{mb}\beta_{bm}f_bE_{I_b} + c\beta_{bm}f_m\Lambda_b + c\beta_{bm}(\mu_m f_b - \mu_b f_m)E_{I_b}}{f_b\Lambda_bE_{I_b} + c\beta_{bm}f_bE_{I_b}I_m}I_m^2 - \frac{(\mu_m f_b - \mu_b f_m)\Lambda_b}{f_b\Lambda_b + c\beta_{bm}f_bI_m}I_m \\ & + \frac{c^2\beta_{mb}\beta_{bm}f_b\Lambda_mE_{I_b}}{(\mu_m f_b - \mu_b f_m)\Lambda_bE_{I_b} + [c\beta_{bm}f_m\Lambda_b + c\beta_{bm}(\mu_m f_b - \mu_b f_m)E_{I_b}]I_m}I_m,\end{aligned} \tag{12}$$

which can be rewritten as

$$\frac{dI_m}{dt} = -\frac{A+B}{C+DI_m}I_m^2 - \frac{E}{C+DI_m}I_m + \frac{A\Lambda_m}{E+BI_m}I_m, \tag{13}$$

where

$$\begin{aligned}&A = c^2\beta_{mb}\beta_{bm}f_bE_{I_b} > 0, \quad B = c\beta_{bm}f_m\Lambda_b + c\beta_{bm}(\mu_m f_b - \mu_b f_m)E_{I_b} > 0, \\ &C = f_b\Lambda_bE_{I_b} > 0, \quad D = c\beta_{bm}f_bE_{I_b} > 0, \quad E = (\mu_m f_b - \mu_b f_m)\Lambda_bE_{I_b}.\end{aligned} \tag{14}$$

Define

$$\begin{aligned}F(I_m) &= -\frac{A+B}{C+DI_m}I_m^2 - \frac{E}{C+DI_m}I_m + \frac{A\Lambda_m}{E+BI_m}I_m \\ &= -\frac{1}{(C+DI_m)(E+BI_m)}I_m[(A+B)BI_m^2 + (AE+2BE-AD\Lambda_m)I_m + E^2 - AC\Lambda_m] \\ &= -\frac{1}{(C+DI_m)(E+BI_m)}I_m h(I_m)\end{aligned} \tag{15}$$

with

$$h(I_m) = (A+B)BI_m^2 + (AE+2BE-AD\Lambda_m)I_m + E^2 - AC\Lambda_m. \tag{16}$$

According to the definition of pseudo-equilibrium of the system (4), which is the equilibrium of $\frac{dI_m}{dt} = F(I_m)$ located in the interior of the sliding segment, we need to find all roots of $F(I_m) = 0$. It is obvious that $I_m = 0$ is one of the roots of $F(I_m) = 0$. To get the other roots of $F(I_m) = 0$, we only need to solve equation $h(I_m) = 0$. Denote $e = (A+B)B$, $f = AE + 2BE - AD\Lambda_m$, $g = E^2 - AC\Lambda_m$, then we get

$$h(I_m) = eI_m^2 + fI_m + g, \tag{17}$$

with $e > 0$ and

$$\begin{aligned}\Delta = f^2 - 4eg &= (AE+2BE-AD\Lambda_m)^2 - 4(A+B)B(E^2 - AC\Lambda_m) \\ &= (AE - AD\Lambda_m)^2 + 4AB\Lambda_m(AC + BC - DE) > 0\end{aligned}$$

due to $AC + BC - DE = c^2\beta_{mb}\beta_{bm}f_b^2\Lambda_bE_{Ib}^2 + c\beta_{bm}f_bf_m\Lambda_b^2E_{Ib} > 0$. Thus equation $h(I_m) = 0$ has two different roots, we denote them by $\tilde{I}_{m1}^*$, $\tilde{I}_{m2}^*$ (suppose $\tilde{I}_{m1}^* < \tilde{I}_{m2}^*$ without loss of generality), and denote the corresponding points on the switching line by $E_1^*(\tilde{I}_{m1}^*, E_{I_b})$, $E_2^*(\tilde{I}_{m2}^*, E_{I_b})$, respectively. To ensure the existence of a pseudo-equilibrium we only need to consider the positive roots of (17) to make sure that the point E_1^* or E_2^* is located in the interior of Σ_S (i.e. inequality $I_{m1} < \tilde{I}_{m1}^* < I_{m2}$ or $I_{m1} < \tilde{I}_{m2}^* < I_{m2}$ holds true). If so, E_1^* or E_2^* is the pseudo-equilibrium, denoted by E_P. To examine the existence of a pseudo-equilibrium we consider the following three cases in terms of the sign of E (defined in (14)).

Case 3.1. $E = 0$, i.e. $\mu_m f_b = \mu_b f_m$.

In such a case ($\mu_m/\mu_b = f_m/f_b$), the ratio of the culling rates of mosquitoes and birds is equivalent to the ratio of their natural death rates. Then the coefficients in (17) satisfy

$$e > 0, \quad f = -AD\Lambda_m < 0, \quad g = -AC\Lambda_m < 0,$$

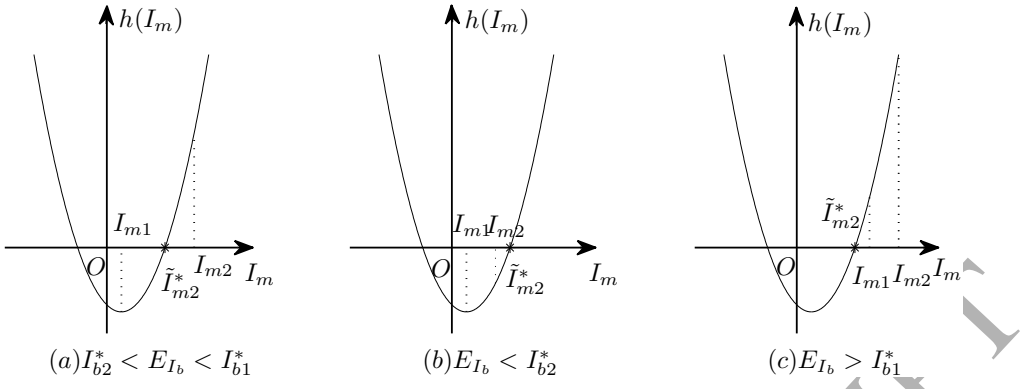

Fig 1: Sketch map of the existence of the pseudo-equilibrium. (a) $I_{m1} < \tilde{I}^*_{m2} < I_{m2}$ if and only if $I^*_{b2} < E_{I_b} < I^*_{b1}$, indicating the existence of the pseudo-equilibrium. (b) $E_{I_b} < I^*_{b2}$ is equivalent to $I_{m1} < I_{m2} < \tilde{I}^*_{m2}$, indicating that the pseudo-equilibrium does not exist. (c) $E_{I_b} > I^*_{b1}$ is equivalent to $I_{m2} > I_{m1} > \tilde{I}^*_{m2}$, indicating that the pseudo-equilibrium does not exist, either.

where A, C, D are defined in (14). Thus there exists one negative root $\tilde{I}^*_{m1} = \frac{-f-\sqrt{f^2-4eg}}{2e}$ and one positive root $\tilde{I}^*_{m2} = \frac{-f+\sqrt{f^2-4eg}}{2e}$ such that $h(I_m) = 0$ holds true. We have the following theorems in terms of whether the point $E^*_2(\tilde{I}^*_{m2}, E_{I_b})$ is in the sliding domain Σ_S.

Theorem 3. *When $R_{02} > 1$, the pseudo-equilibrium $E_P(\tilde{I}^*_{m2}, E_{I_b})$ exists if and only if $I^*_{b2} < E_{I_b} < I^*_{b1}$.*

Proof. If $R_{02} > 1$, both endemic equilibria E_1 and E_2 of the two subsystems are feasible. Substituting I_{m1} into $h(I_m)$ and simplifying give

$$h(I_{m1}) = \frac{\Lambda_b^2 E_{I_b}^2}{(\Lambda_b - \mu_b E_{I_b})^2}[(c^2\beta_{mb}\beta_{bm}\mu_b f_b^2\Lambda_m + c\beta_{mb}\mu_b^2 f_b f_m \Lambda_b)E_{I_b} - (c^2\beta_{mb}\beta_{bm}f_b^2\Lambda_m\Lambda_b - \mu_b^2 f_m^2\Lambda_b^2)]. \tag{18}$$

Thus we have

$$h(I_{m1}) < 0 \;\Leftrightarrow\; E_{I_b} < \frac{c^2\beta_{mb}\beta_{bm}f_b^2\Lambda_m\Lambda_b - \mu_b^2 f_m^2\Lambda_b^2}{c^2\beta_{mb}\beta_{bm}\mu_b f_b^2\Lambda_m + c\beta_{mb}\mu_b^2 f_b f_m\Lambda_b} = I^*_{b1}. \tag{19}$$

Similarly,

$$\begin{aligned} h(I_{m2}) \;&= \frac{\Lambda_b^2 E_{I_b}^2}{[\Lambda_b - (\mu_b+f_b)E_{I_b}]^2} \\ &\cdot[(c^2\beta_{mb}\beta_{bm}(\mu_b+f_b)f_b^2\Lambda_m + c\beta_{mb}(\mu_b+f_b)^2 f_b f_m\Lambda_b)E_{I_b} - (c^2\beta_{mb}\beta_{bm}f_b^2\Lambda_m\Lambda_b - (\mu_b+f_b)^2 f_m^2\Lambda_b^2)], \end{aligned} \tag{20}$$

and

$$h(I_{m2}) > 0 \Leftrightarrow E_{I_b} > \frac{c^2\beta_{mb}\beta_{bm}f_b^2\Lambda_m\Lambda_b - (\mu_b+f_b)^2 f_m^2\Lambda_b^2}{c^2\beta_{mb}\beta_{bm}(\mu_b+f_b)f_b^2\Lambda_m + c\beta_{mb}(\mu_b+f_b)^2 f_b f_m\Lambda_b} = I^*_{b2}. \tag{21}$$

Thus

$$h(I_{m1}) < 0 < h(I_{m2}) \Leftrightarrow I^*_{b2} < E_{I_b} < I^*_{b1}. \tag{22}$$

Note that $h(I_m)$ is a quadratic function about I_m whose graph is a curved shape opening up, with $g = h(0) < 0$ and $\tilde{I}^*_{m2}$ is the positive root satisfying $h(\tilde{I}^*_{m2}) = 0$, we have

$$h(I_{m1}) < 0 = h(\tilde{I}^*_{m2}) < h(I_{m2}) \Leftrightarrow I_{m1} < \tilde{I}^*_{m2} < I_{m2}. \tag{23}$$

It is easy to see that $I_{m1} < \tilde{I}^*_{m2} < I_{m2} \Leftrightarrow h(I_{m1}) < 0 < h(I_{m2}) \Leftrightarrow I^*_{b2} < E_{I_b} < I^*_{b1}$. So the pseudo-equilibrium $E_P(\tilde{I}^*_{m2}, E_{I_b})$ exists if and only if $I^*_{b2} < E_{I_b} < I^*_{b1}$, as indicated in Fig 1(a). This completes the proof.

When $R_{02} < 1 < R_{01}$, the endemic equilibrium of the $free-system$ exists while the endemic equilibrium of the $control-system$ does not exist. By similar analysis to that in the proof of Theorem 3, we have the following

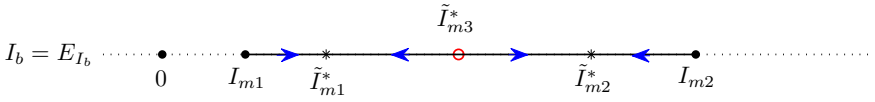

Fig 2: Sketch map of the impossibility of the existence of two pseudo-equilibria on the switching line.

conclusion.

Theorem 4. *When $R_{02} < 1 < R_{01}$, the pseudo-equilibrium $E_P(\tilde{I}^*_{m2}, E_{I_b})$ exists if and only if $E_{I_b} < I^*_{b1}$.*

Case 3.2. $E > 0$, i.e. $\mu_m f_b > \mu_b f_m$.

In such a case ($\mu_m/\mu_b > f_m/f_b$), the ratio of the culling rates of mosquitoes and birds is less than the ratio of their natural death rates. Then we have $e > 0,\ \frac{\mu_b f_m}{\mu_m f_b} < 1,\ (1-\frac{\mu_b f_m}{\mu_m f_b})^2 < 1$.

Note that $R_{01} > 1 > (1-\frac{\mu_b f_m}{\mu_m f_b})^2$, which means that $g = \mu_m^2 f_b^2 \Lambda_b^2 E_{I_b}^2[(1-\frac{\mu_b f_m}{\mu_m f_b})^2 - R_{01}] < 0$, indicating that $h(I_m) = 0$ has one negative root $\tilde{I}^*_{m1} = \frac{-f-\sqrt{f^2-4eg}}{2e}$ and one positive root $\tilde{I}^*_{m2} = \frac{-f+\sqrt{f^2-4eg}}{2e}$. Similarly to the analysis in the case of $E = 0$, to ensure that $I_{m1} < \tilde{I}^*_{m2} < I_{m2}$, $h(I_m)$ should satisfy : $h(I_{m1}) < 0 < h(I_{m2})$, which is equivalent to $I^*_{b2} < E_{I_b} < I^*_{b1}$. When $R_{02} < 1 < R_{01}$, the endemic equilibrium of the $free-system$ exists while the endemic equilibrium of the $control-system$ does not exist, which illustrates that the pseudo-equilibrium $E_P(\tilde{I}^*_{m2}, E_{I_b})$ exists if and only if $E_{I_b} < I^*_{b1}$. Therefore, the pseudo-equilibrium $E_P(\tilde{I}^*_{m2}, E_{I_b})$ is feasible if and only if $I^*_{b2} < E_{I_b} < I^*_{b1}$ for $R_{02} > 1$ or $E_{I_b} < I^*_{b1}$ for $R_{02} < 1$.

Case 3.3. $E < 0$, i.e. $\mu_m f_b < \mu_b f_m$.

In this scenario ($\mu_m/\mu_b < f_m/f_b$), the ratio of the culling rates of mosquitoes and birds is greater than the ratio of their natural death rates. Then we have $e > 0,\ f = AE + 2BE - AD\Lambda_m < 0,\ \frac{\mu_b f_m}{\mu_m f_b} > 1$. We consider the following two situations in terms of the number of roots of equation $h(I_m) = 0$:

(1) When $1 < R_{01} < (1-\frac{\mu_b f_m}{\mu_m f_b})^2$, $g > 0$ holds true, there exist two positive roots of $h(I_m) = 0$, namely, $\tilde{I}^*_{m1} = \frac{-f-\sqrt{f^2-4eg}}{2e}, \tilde{I}^*_{m2} = \frac{-f+\sqrt{f^2-4eg}}{2e}$. Initially we will show that it is impossible to have two pseudo-equilibria. Suppose that there are two pseudo-equilibria, namely, $I_{m1} < \tilde{I}^*_{m1} < \tilde{I}^*_{m2} < I_{m2}$ holds true. Calculating the derivative of $F(I_m)$ with respect to I_m at the pseudo-equilibrium $(\tilde{I}^*_m, E_{I_b})$ gives

$$F'(\tilde{I}^*_m) = -[\frac{AC+BC-DE}{(C+D\tilde{I}^*_m)^2} + \frac{AB\Lambda_m}{(E+B\tilde{I}^*_m)^2}]\tilde{I}^*_m < 0. \tag{24}$$

It means that $F'(\tilde{I}^*_{m1}) < 0, F'(\tilde{I}^*_{m2}) < 0$ both hold true, meaning the local stability of both E^*_1 and E^*_2. Then there must exist at least one other unstable equilibrium $E^*_3(\tilde{I}^*_{m3}, E_{I_b})$ located in between E^*_1 and E^*_2, i.e. $\tilde{I}^*_{m1} < \tilde{I}^*_{m3} < \tilde{I}^*_{m2}$, as shown in Fig 2. This contradicts the fact that there are only two roots of $h(I_m) = 0$ at most. Hence it is impossible to have two pseudo-equilibria.

Suppose only point $E^*_1(\tilde{I}^*_{m1}, E_{I_b})$ is the pseudo-equilibrium, then $I_{m1} < \tilde{I}^*_{m1} < I_{m2} < \tilde{I}^*_{m2}$ holds true, which means that $h(I_{m1}) > 0, h(I_{m2}) < 0$, being equivalent to $I^*_{b1} < E_{I_b} < I^*_{b2}$ from the previous calculation, which contradicts $I^*_{b2} < I^*_{b1}$. Hence E^*_1 cannot be a pseudo-equilibrium. If point $E^*_2(\tilde{I}^*_{m2}, E_{I_b})$ is a pseudo-equilibrium, i.e. $\tilde{I}^*_{m1} < I_{m1} < \tilde{I}^*_{m2} < I_{m2}$, which means that $h(I_{m1}) < 0, h(I_{m2}) > 0$, being equivalent to $I^*_{b2} < E_{I_b} < I^*_{b1}$. Thus, we get that when $1 < R_{01} < (1-\frac{\mu_b f_m}{\mu_m f_b})^2$, there exists one pseudo-equilibrium $E_P(\tilde{I}^*_{m2}, E_{I_b})$ if and only if $I^*_{b2} < E_{I_b} < I^*_{b1}$.

(2) When $R_{01} \geq (1-\frac{\mu_b f_m}{\mu_m f_b})^2$, we have $g \leq 0$, and then equation $h(I_m) = 0$ has one non-positive root $\tilde{I}^*_{m1} = \frac{-f-\sqrt{f^2-4eg}}{2e}$ and one positive root $\tilde{I}^*_{m2} = \frac{-f+\sqrt{f^2-4eg}}{2e}$. To ensure the existence of the pseudo-equilibrium $E_P(\tilde{I}^*_{m2}, E_{I_b})$, inequality $I_{m1} < \tilde{I}^*_{m2} < I_{m2}$ should be satisfied, which means that $h(I_m)$ should satisfy $h(I_{m1}) < 0$ and $h(I_{m2}) > 0$, being equivalent to $I^*_{b2} < E_{I_b} < I^*_{b1}$. Hence, $E^*_2(\tilde{I}^*_{m2}, E_{I_b})$ is the unique pseudo-equilibrium for $I^*_{b2} < E_{I_b} < I^*_{b1}$, denoted by E_P.

For the Case 3.3 we conclude that if $I^*_{b2} < E_{I_b} < I^*_{b1}$ then $E_P(\tilde{I}^*_{m2}, E_{I_b})$ is the unique pseudo-equilibrium.

We summarize the existence of endemic equilibria for system (5) and system (9) and the pseudo-equilibrium of system (4) in Table 2.

Table 2: Existence of equilibria of the system (4) when $R_{01} > 1$

Range of parameter values	Existence of regular equilibria	Existence of Pseudo-equilibrium	
		Range of the threshold	Pseudo-equilibrium
$R_{01} > R_{02} > 1$	E_1, E_2	$E_{I_b} < I^*_{b2}$	Non-existent
		$I^*_{b2} < E_{I_b} < I^*_{b1}$	$E_P(E^*_2)$
		$E_{I_b} > I^*_{b1}$	Non-existent
$R_{01} > 1 > R_{02}$	E_1	$0 < E_{I_b} < I^*_{b1}$	$E_P(E^*_2)$
		$E_{I_b} > I^*_{b1}$	Non-existent

4. Boundary node bifurcation analysis

After investigating the regular equilibrium and pseudo-equilibrium, we note that when the threshold E_{I_b} is chosen as the critical value, endemic equilibrium E_1 (E_2) may collide with the pseudo-equilibrium E_P and the left (right) endpoint T_1 (T_2) of the sliding segment $\overline{T_1T_2}$, and consequently bifurcation occurs.

We shall investigate the boundary node bifurcation in the following. Initially, two types of special point: the tangent point and the boundary equilibrium, excluding the regular equilibrium and the pseudo-equilibrium, are discussed.

The tangent point of system (4) is defined as a point E_T where the vectors $F_i(E_T)(i = 1,2)$ are nonzero but either $F_1(X)$ or $F_2(X)$ is tangent to the switching line Σ at point E_T, namely, $\langle F_1(E_T), H_X(E_T)\rangle = 0$ or $\langle F_2(E_T), H_X(E_T)\rangle = 0$. Thus the tangent points of system (3) with (2) satisfy:

$$c\beta_{bm}(1 - \tfrac{(\mu_b+\varepsilon f_b)I_b}{\Lambda_b})I_m - (\mu_b + \varepsilon f_b)I_b = 0, \;\; I_b = E_{I_b}. \tag{25}$$

We have the following two tangent points: $E_{T_1}(I_{m1}, E_{I_b}), E_{T_2}(I_{m2}, E_{I_b})$. It is clear that two tangent points E_{T_1} and E_{T_2} are the endpoints T_1 and T_2 of the sliding domain Σ_S and we denote them by T_1 and T_2 in the following for convenience.

The boundary equilibrium of system (4) is the equilibrium E_B of the sliding mode where $F_1(E_B) = 0$ or $F_2(E_B) = 0$. Thus the boundary equilibrium of system (3) with (2) satisfies:

$$\begin{cases} c\beta_{mb}\frac{(\mu_b+\varepsilon f_b)I_b}{\Lambda_b}(\frac{\Lambda_m}{(\mu_m+\varepsilon f_m)} - I_m) - (\mu_m + \varepsilon f_m)I_m = 0, \\ c\beta_{bm}(1 - \frac{(\mu_b+\varepsilon f_b)I_b}{\Lambda_b})I_m - (\mu_b + \varepsilon f_b)I_b = 0, \\ I_b - E_{I_b} = 0. \end{cases} \tag{26}$$

Then the following equality

$$\frac{c\beta_{mb}\frac{(\mu_b+\varepsilon f_b)E_{I_b}\Lambda_m}{(\mu_m+\varepsilon f_m)\Lambda_b}}{c\beta_{mb}\frac{(\mu_b+\varepsilon f_b)E_{I_b}}{\Lambda_b} + (\mu_m+\varepsilon f_m)} = \frac{(\mu_b+\varepsilon f_b)E_{I_b}}{c\beta_{bm}(1-\frac{(\mu_b+\varepsilon f_b)E_{I_b}}{\Lambda_b})} \tag{27}$$

where $\varepsilon = 0, 1$, should be established to ensure the existence of the boundary equilibrium, which indicates that $E_{I_b} = I^*_{b1}$ for $\varepsilon = 0$ while $E_{I_b} = I^*_{b2}$ for $\varepsilon = 1$. Hence, there exists a boundary equilibrium $E^1_B(I^*_{m1}, E_{I_b})$ or $E^2_B(I^*_{m2}, E_{I_b})$ which is the endemic equilibrium E_1 (when $E_{I_b} = I^*_{b1}$) or E_2 (when $E_{I_b} = I^*_{b2}$), respectively.

Boundary node bifurcation occurs if the node, tangent point and pseudo-equilibrium collide when the threshold parameter E_{I_b} is chosen as a specific value. If $R_{02} > 1$, the endemic equilibrium E_1 (E_2) may collide with the pseudo-equilibrium E_P and the left (right) endpoint T_1 (T_2) of the sliding segment $\overline{T_1T_2}$ (namely, the tangent point), when $E_{I_b} = I^*_{b1}$ ($E_{I_b} = I^*_{b2}$), and in such case, the collision point is an attractor (shown in Fig 3(b)). If $R_{02} < 1 < R_{01}$, the collision of points E_1, E_P and T_1 occurs when $E_{I_b} = I^*_{b1}$, and the collision point is an attractor. For example, Fig 3 shows the boundary node bifurcation as the parameter E_{I_b} increases. The virtual equilibrium E^V_1, the tangent point T_1 and the stable pseudo-equilibrium E_P coexist for $E_{I_b} < I^*_{b1}$, as shown in Fig 3(a) with $E_{I_b} = 1.0$. They collide at

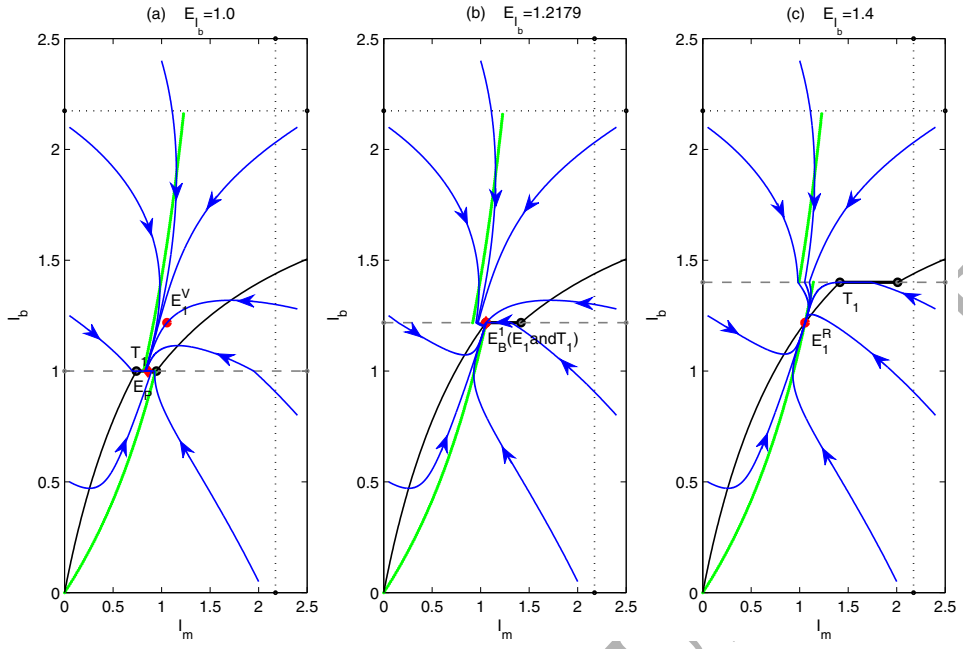

Fig 3: Boundary node bifurcation for system (4). Parameter E_{I_b} is chosen as the bifurcation parameter and other parameter values are fixed as $c = 10, \mu_m = 2, \mu_b = 0.8, \beta_{mb} = 0.3, \beta_{bm} = 0.18, f_m = 0.3, f_b = 0.12, \Lambda_m = 5, \Lambda_b = 2$. (a) $E_{I_b} = 1.0$, (b) $E_{I_b} = 1.2179$, (c) $E_{I_b} = 1.4$.

$E_{I_b} = I^*_{b1} = 1.2179$, becoming a boundary equilibrium E^1_B, as shown in Fig 3(b) and are substituted by a real equilibrium E^R_1 and a tangent point T_1 for $E_{I_b} > I^*_{b1}$, as shown in Fig 3(c) with $E_{I_b} = 1.4$. The occurring of the bifurcation shows how a stable pseudo-equilibrium disappears and becomes a stable node. Another boundary node bifurcation occurs when parameter E_{I_b} varies by passing through the critical level I^*_{b2} when $R_{02} > 1$. In such case, the stable node E^R_2 and the tangent point T_2 coexist for $E_{I_b} < I^*_{b2}$, collide at $E_{I_b} = I^*_{b2}$ and are replaced by a pseudo-equilibrium E_P and a tangent point T_2 for $E_{I_b} > I^*_{b2}$. In Fig 3, solid thick black segments represent the sliding segments, red cycle points denote the regular or virtual equilibria, red rhombus points represent the pseudo-equilibrium, black cycle points denotes the tangent points, green solid curves represent vertical null-isoclines and black solid curves denote the horizontal null-isoclines, blue solid curves represent trajectories. Note that, unless otherwise stated, we use this notation throughout the rest of this paper.

5. Global behaviour of the system

We initially investigate the global dynamics of the system (4) with (2) under different threshold levels when $R_{02} > 1$. By using a similar method to the above we can get a conclusion for the case of $R_{01} > 1 > R_{02}$.

We will examine the global stability by ruling out the existence of limit cycles. By formulating the suitable Dulac function $\mathscr{B} = \frac{1}{I_m I_b}$, we have obtained the global stability of the positive equilibria of system (5) in region Ω_1 and system (9) in region Ω_2. Therefore we have the following Lemma 1. Then we shall discuss the existence of limit cycles which contain part of the sliding domain or surround the sliding segment.

Lemma 1. *There is no limit cycle which is totally in region Ω_1 or Ω_2.*

Lemma 2. *There is no limit cycle which contains part of the sliding domain Σ_S.*

Proof. For $E_{I_b} < I^*_{b2}$, we know that the equilibrium $E_2(I^*_{m2}, I^*_{b_2})$ is a real equilibrium and stable node, denoted by $E^R_2(I^*_{m2}, I^*_{b_2})$. Moreover, we have $h(I_m) < 0$ for $I_{m1} < I_m < I_{m2}$, thus $F(I_m) > 0$, namely, the sliding mode dynamics

(12) satisfy $\frac{dI_m}{dt} > 0$, which means that the trajectory moves from the left to the right on the sliding segment $\overline{T_1T_2}$. Suppose that there exists a closed orbit containing part of the sliding segment $\overline{T_1T_2}$, then the closed orbit must go through the point T_2. While any trajectory starting from the tangent point T_2 will approach $E_2^R(I_{m2}^*, I_{b_2}^*)$ directly without hitting the manifold Σ since $E_2^R(I_{m2}^*, I_{b_2}^*)$ is a stable node, as shown in Fig 4(a), this contradicts the existence of the closed orbit going through the point T_2. Therefore, no closed orbit containing part of the sliding segment $\overline{T_1T_2}$ exists. When $I_{b2}^* < E_{I_b} < I_{b1}^*$, we get that there exists only one pseudo-equilibrium, and it is locally stable in the sliding domain because $F'(\tilde{I}_{m2}^*) < 0$ shown in (24). This indicates that any orbit, once reaching the sliding domain at some time, will slide towards the pseudo-equilibrium. Then, we obtain that no limit cycle containing part of the sliding domain exists when $I_{b2}^* < E_{I_b} < I_{b1}^*$. For $E_{I_b} > I_{b1}^*$, the equilibrium $E_1(I_{m1}^*, I_{b_1}^*)$ is a real equilibrium and stable node. The sliding mode dynamics (12) satisfy $\frac{dI_m}{dt} < 0$, indicating that the trajectory moves from the right to the left on the sliding segment $\overline{T_1T_2}$, then we can use a similar process as for the case of $E_{I_b} < I_{b2}^*$ to prove the nonexistence of the closed orbit containing part of the switching segment $\overline{T_1T_2}$. This completes the proof.

Lemma 3. *There is no limit cycle surrounding the sliding segment* $\overline{T_1T_2}$.

Proof. Suppose that there exists a limit cycle Γ that passes through the discontinuous manifold Σ and contains the sliding domain Σ_S in its interior with period ω, shown in Fig 4(b). Denote its part below the line $I_b = E_{I_b}$ by Γ_1 and its part above the line $I_b = E_{I_b}$ by Γ_2. Denote the intersection points of the limit cycle Γ and the line $I_b = E_{I_b}$ by P and Q, the intersection points of Γ and the auxiliary line $I_b = E_{I_b} - \delta$ by P_1 and Q_1, and the intersection points of Γ and another auxiliary line $I_b = E_{I_b} + \delta$ by P_2 and Q_2, where $\delta > 0$ is sufficiently small. Let G_1 be the region delimited by Γ_1 and the segment P_1Q_1, G_2 be the region delimited by Γ_2 and the segment P_2Q_2. Denote the boundary of G_1 and G_2 by L_1 and L_2, respectively. Moreover, Suppose that the abscissas of the points P, Q, P_1, Q_1, P_2, Q_2 are $\underline{I}_m, \bar{I}_m, \underline{I}_m + a_1(\delta), \bar{I}_m - b_1(\delta), \underline{I}_m + a_2(\delta), \bar{I}_m - b_2(\delta)$, respectively, where $\underline{I}_m < \bar{I}_m$ and $a_i(\delta), b_i(\delta)$ is continuous with respect to δ and satisfies $\lim_{\delta\to 0} a_i(\delta) = \lim_{\delta\to 0} b_i(\delta) = 0$ for $i = 1, 2$. Let the Dulac function be $\mathscr{B} = \frac{1}{I_m I_b}$ defined as before. By the discussion given above and Green's theorem, we obtain the following:

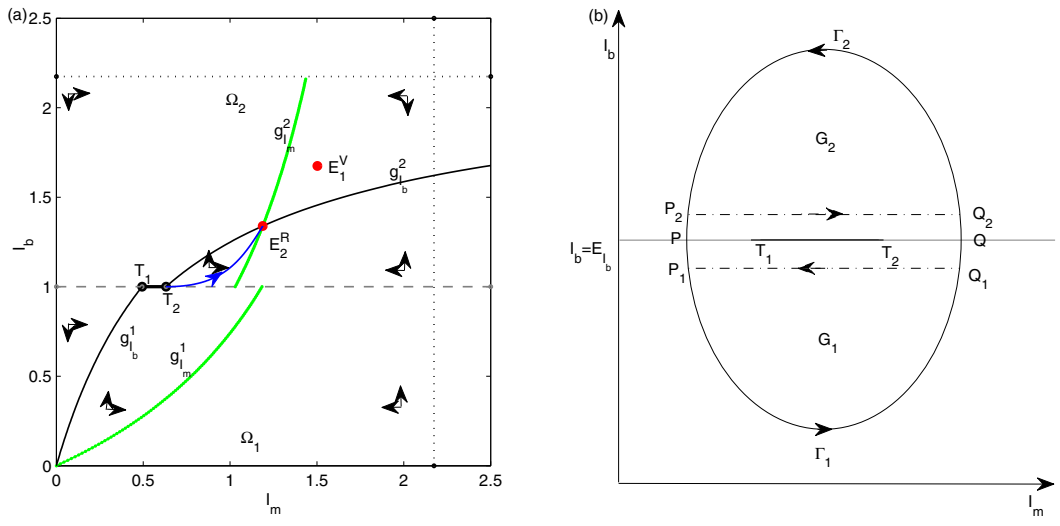

Fig 4: (a) Phase plane $I_m - I_b$ for system (4), showing the switching line $I_b = E_{I_b}$, sliding segment $\overline{T_1T_2}$, virtual equilibrium (solid circle: E_1^V), real equilibrium (solid circle: E_2^R). The horizonal isoclinic curve (black) $g_{I_b}^1(g_{I_b}^2)$ and the vertical isoclinic curve (green) $g_{I_m}^1(g_{I_m}^2)$ are plotted for the free (control) system, respectively. The blue curve represents the orbit starting from T_2 in the phase plane indicating the stable node E_2^R, excluding the existence of closed orbit containing part of the switching segment $\overline{T_1T_2}$. (b) Schematic diagram illustrating the nonexistence of the closed trajectory of the system (4) surrounding the sliding segment $\overline{T_1T_2}$.

$$\begin{aligned}\iint_{G_1}[\tfrac{\partial(\mathscr{B}F_{11})}{\partial I_m}+\tfrac{\partial(\mathscr{B}F_{12})}{\partial I_b}]dI_mdI_b &= \oint_{L_1}(\mathscr{B}F_{11}dI_b-\mathscr{B}F_{12}dI_m)\\ &= \int_{\Gamma_1}(\mathscr{B}F_{11}F_{12}-\mathscr{B}F_{12}F_{11})dt-\int_{\overrightarrow{Q_1P_1}}\mathscr{B}F_{12}dI_m\\ &= -\int_{\overrightarrow{Q_1P_1}}\mathscr{B}F_{12}dI_m,\end{aligned} \tag{28}$$

$$\begin{aligned}\iint_{G_2}[\tfrac{\partial(\mathscr{B}F_{21})}{\partial I_m}+\tfrac{\partial(\mathscr{B}F_{22})}{\partial I_b}]dI_mdI_b &= \oint_{L_2}(\mathscr{B}F_{21}dI_b-\mathscr{B}F_{22}dI_m)\\ &= \int_{\Gamma_2}(\mathscr{B}F_{21}F_{22}-\mathscr{B}F_{22}F_{21})dt-\int_{\overrightarrow{P_2Q_2}}\mathscr{B}F_{22}dI_m\\ &= -\int_{\overrightarrow{P_2Q_2}}\mathscr{B}F_{22}dI_m,\end{aligned} \tag{29}$$

Suppose $G_{10}\subset G_1$, then

$$\xi=\iint_{G_{10}}[\tfrac{\partial(\mathscr{B}F_{11})}{\partial I_m}+\tfrac{\partial(\mathscr{B}F_{12})}{\partial I_b}]dI_mdI_b<0, \tag{30}$$

furthermore,

$$0>\xi>\iint_{G_1}\tfrac{\partial(\mathscr{B}F_{11})}{\partial I_m}+\tfrac{\partial(\mathscr{B}F_{12})}{\partial I_b}dI_mdI_b+\iint_{G_2}\tfrac{\partial(\mathscr{B}F_{21})}{\partial I_m}+\tfrac{\partial(\mathscr{B}F_{22})}{\partial I_b}dI_mdI_b, \tag{31}$$

which means that

$$0>\xi>-\int_{\overrightarrow{Q_1P_1}}\mathscr{B}F_{12}dI_m-\int_{\overrightarrow{P_2Q_2}}\mathscr{B}F_{22}dI_m, \tag{32}$$

By taking the limit $\delta\to 0$, we get

$$\begin{aligned}&\lim_{\delta\to0}(-\int_{\overrightarrow{Q_1P_1}}\mathscr{B}F_{12}dI_m-\int_{\overrightarrow{P_2Q_2}}\mathscr{B}F_{22}dI_m)\\ &=\lim_{\delta\to0}[\int_{\underline{I}_m+a_1(\delta)}^{\bar{I}_m-b_1(\delta)}(c\beta_{bm}\tfrac{1}{E_{I_b}-\delta}-c\beta_{bm}\tfrac{\mu_b}{\Lambda_b}-\tfrac{\mu_b}{I_m})dI_m-\int_{\underline{I}_m+a_2(\delta)}^{\bar{I}_m-b_2(\delta)}(c\beta_{bm}\tfrac{1}{E_{I_b}+\delta}-c\beta_{bm}\tfrac{\mu_b+f_b}{\Lambda_b}-\tfrac{\mu_b+f_b}{I_m})dI_m]\\ &=\lim_{\delta\to0}[(c\beta_{bm}\tfrac{1}{E_{I_b}-\delta}-c\beta_{bm}\tfrac{\mu_b}{\Lambda_b})(\bar{I}_m-b_1(\delta)-\underline{I}_m-a_1(\delta))-\mu_b\ln|\tfrac{\bar{I}_m-b_1(\delta)}{\underline{I}_m+a_1(\delta)}|\\ &\quad-(c\beta_{bm}\tfrac{1}{E_{I_b}+\delta}-c\beta_{bm}\tfrac{\mu_b+f_b}{\Lambda_b})(\bar{I}_m-b_2(\delta)-\underline{I}_m-a_2(\delta))+(\mu_b+f_b)\ln|\tfrac{\bar{I}_m-b_2(\delta)}{\underline{I}_m+a_2(\delta)}|]\\ &=c\beta_{bm}\tfrac{f_b}{\Lambda_b}(\bar{I}_m-\underline{I}_m)+f_b\ln|\tfrac{\bar{I}_m}{\underline{I}_m}|\\ &>0.\end{aligned} \tag{33}$$

which contradicts (32). Thus there is no limit cycle surrounding the sliding segment $\overline{T_1T_2}$.

To present all possible dynamic behaviour of the system (4) with (2), we choose different values of the parameters such that the dynamics in all regions are exhibited.

Theorem 5. *The equilibrium E_1^R is globally asymptotically stable if $E_{I_b}>I_{b1}^*$.*

Proof. We initially consider $R_{02}>1$. Then the endemic equilibrium E_1 is real and E_2 is a virtual equilibrium for $E_{I_b}>I_{b1}^*$, denoted by E_1^R and E_2^V, respectively. And there is no pseudo-equilibrium according to the above calculation for $E_{I_b}>I_{b1}^*$. It has been proved that the endemic equilibria E_1^R and E_2^V are both locally asymptotically stable nodes. Note that a limit cycle totally located in the region Ω_1 and Ω_2 does not exist by Lemma 1. Hence, trajectories initiating from region Ω_1 will either tend to equilibrium E_1^R directly or hit the sliding domain and move from the right to the left endpoint T_1 along the sliding segment, or enter the region Ω_2 by crossing through the crossing segment. While trajectories initiating from region Ω_2 will either hit the sliding domain and then move from the right to the left endpoint T_1 along the sliding segment or enter the region Ω_1 by crossing through the crossing segment in order to approach E_2^V (shown in Fig 5(a)). Moreover, Lemma 2 and Lemma 3 exclude the existence of limit cycles which contain the part of the sliding segment or surround the sliding segment $\overline{T_1T_2}$. Thus, all trajectories ultimately tend to E_1^R. Hence, a combination of Lemma 1, Lemma 2 and Lemma 3 implies that E_1^R is globally asymptotically stable. For the case of $R_{01}>1>R_{02}$, we can also get the global stability by using similar analysis.

Theorem 6. *The pseudo-equilibrium E_P is globally asymptotically stable if* $\max\{0, I^*_{b2}\} < E_{I_b} < I^*_{b1}$.

Proof. Suppose $R_{02} > 1$ initially, then $I^*_{b2} > 0$. We know that for $I^*_{b2} < E_{I_b} < I^*_{b1}$, both locally stable equilibria E_1 and E_2 are located in their opposite regions and are virtual equilibria (denoted by E^V_1 and E^V_2, respectively), so they cannot be reached. Consequently, any trajectory initiating from region Ω_1 (Ω_2) will reach the switching line in order to approach the equilibrium E^V_1 (E^V_2) located in Ω_2 (Ω_1) (shown in Fig 5(b)). Note that the pseudo-equilibrium E_P exists and is stable in the sliding domain. If the intersecting point is in the sliding segment, then the trajectory will move to pseudo-equilibrium E_P; if the intersecting point is in the crossing segment, no limit cycle exists according to Lemma 1-3, thus the trajectory will hit the sliding segment sooner or later and then slide to the pseudo-equilibrium E_P. Hence, we conclude that the pseudo-equilibrium E_P is globally asymptotically stable. For the case of $R_{01} > 1 > R_{02}$, we know that $I^*_{b2} < 0$, and in such case a similar analysis yields the global stability of E_P when $0 < E_{I_b} < I^*_{b1}$, as shown in Fig 5(d).

When $R_{02} > 1$, we know that the endemic equilibrium E_1 is virtual (denoted by E^V_1) and E_2 is a real equilibrium (denoted by E^R_2) for $E_{I_b} < I^*_{b2}$. In such case, no pseudo-equilibrium exists and any trajectory which reaches the sliding segment will move from the left to the right on the sliding segment (shown in Fig 5(c)). By a similar discussion to the proof of Theorem 5, we know that E^R_2 is globally asymptotically stable and have the following conclusion.

Theorem 7. *The equilibrium E^R_2 is globally asymptotically stable if $E_{I_b} < I^*_{b2}$.*

In summary, system (4) is proposed as a system with piecewise constant culling rates. It follows from Theorems 5 - 7 that the solutions of the system (4) ultimately converge to either one of two endemic equilibria (i.e. E_1 or E_2) for two structures or the pseudo-equilibrium E_P in the sliding domain, depending on the different choices of the critical level E_{I_b}. The most interesting and important case is that the system (4) can stabilize at the pseudo-equilibrium E_P (Theorem 6), which is new and qualitatively different from the equilibrium for the control system (9).

6. Conclusion and Discussion

A few mathematical models have discussed the impact of control strategies, such as mosquito reduction mechanisms and personal protection against exposure to mosquitoes, on the transmission dynamics of WNV [4, 6, 10, 13, 20, 22]. The previously formulated models implicitly assume that the control occurs throughout all of the epidemic period or only at some fixed points. However, a lot of material and financial resources are needed to measure the number of infected mosquitoes, and the public or responsible authority cannot be aware of the transmission of WNV when the number of infected birds is usually small at the initial stages when WNV starts to spread. So we have proposed a mathematical model of WNV transmission with piecewise constant culling rates of mosquitoes and birds to represent a culling control strategy that is implemented once the number of infected birds exceeds a certain level while no control is carried out otherwise.

We call the piecewise smooth ordinary differential equation model (4) presented in this paper a system with a Filippov-type control, and the solution of system (4) is composed of the solutions of the $free-system$, $control-system$ and the sliding dynamics. The global properties of the Filippov model were investigated and all possible dynamic behaviour that the proposed model can exhibit are presented, as can be seen in Fig 5(a)-(d). Our findings suggest that the system stabilizes at the equilibrium point E^R_1, E^R_2, or E_P, depending on the threshold level E_{I_b}. Different values of the threshold level E_{I_b} were chosen to show different dynamic behaviour. For example, Fig 5(a) shows that when $E_{I_b} > I^*_{b1}$, endemic equilibrium E^R_1 is globally asymptotically stable. Similarly, Fig 5(c) shows that endemic equilibrium E^R_2 is globally asymptotically stable when $E_{I_b} < I^*_{b2}$. The most interesting case occurs in Fig 5(b), in which the pseudo-equilibrium induced by the threshold policy exists and is globally asymptotically stable. In such a case, the threshold level E_{I_b} is in between I^*_{b2} and I^*_{b1} (i.e. $I^*_{b2} < E_{I_b} < I^*_{b1}$) and both the equilibria E_1 and E_2 are virtual. Furthermore, the global stability of the pseudo-equilibrium implies that the number of infected birds can

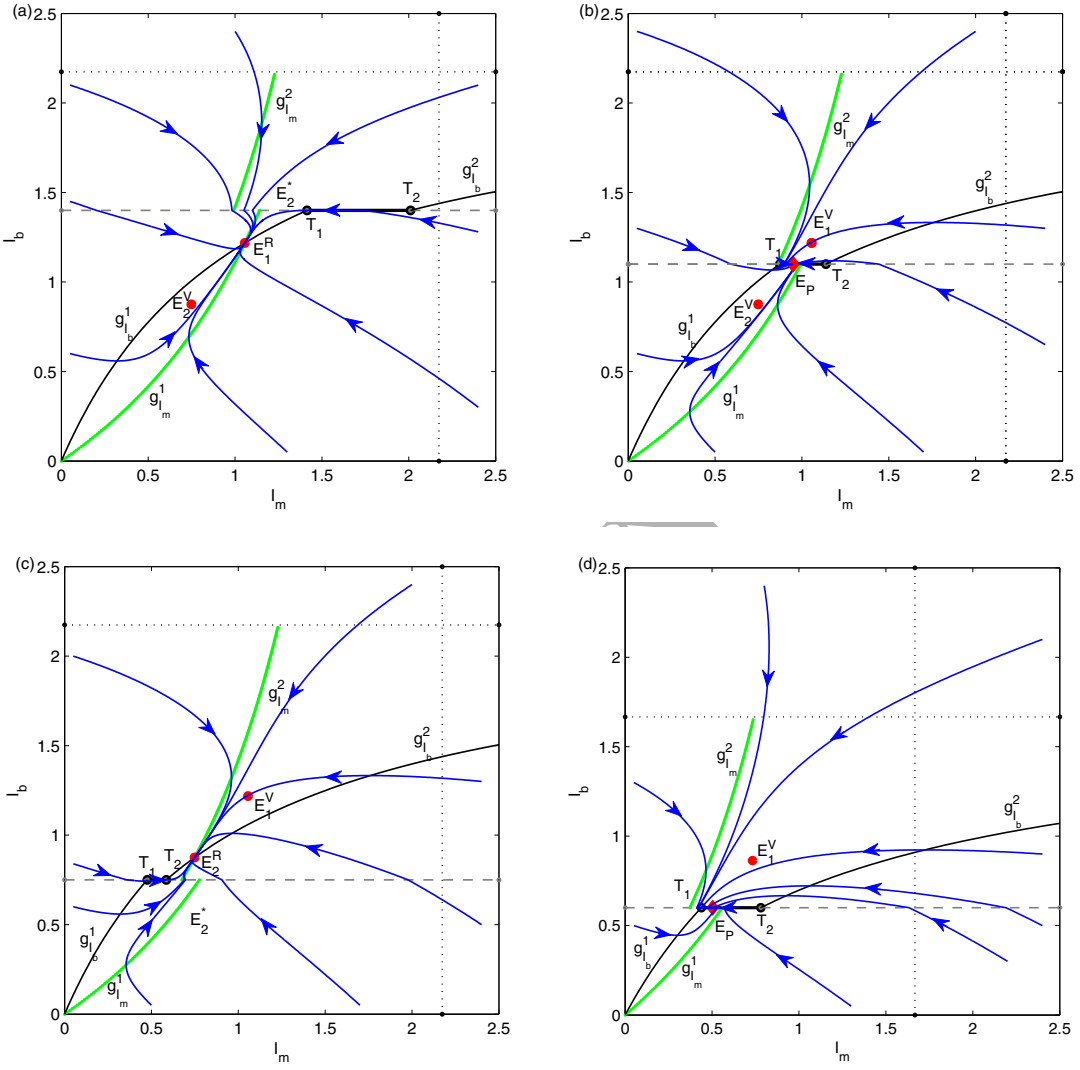

Fig 5: (a)-(d) are phase planes $I_m - I_b$ for system (4), showing the sliding domain $\overline{T_1T_2}$, asymptotic equilibrium including real equilibrium (solid circles: E_1^R or E_2^R), virtual equilibrium (solid circles: E_1^V or E_2^V) and pseudo-equilibrium (solid rhombus: E_P), for different threshold values. The blue curves represent the orbits in the phase plane indicating the asymptotic equilibrium. (a)-(c) show the global stability of system (4) when $R_{01} > R_{02} > 1$. Parameters values are $c = 10, \mu_m = 2, \mu_b = 0.8, \beta_{mb} = 0.3, \beta_{bm} = 0.18, f_m = 0.3, f_b = 0.12, \Lambda_m = 5, \Lambda_b = 2$ such that $R_{01} = 3.375 > R_{02} = 2.552 > 1$, and the threshold parameter is chosen as follows: (a) $E_{I_b} = 1.4$ such that $E_{I_b} > I^*_{b1} > I^*_{b2}$, and E_1^R is globally asymptotically stable; (b) $E_{I_b} = 1.1$ such that $I^*_{b2} < E_{I_b} < I^*_{b1}$, E_P exists and is globally asymptotically stable; (c) $E_{I_b} = 0.75$ such that $E_{I_b} < I^*_{b2} < I^*_{b1}$, and E_2^R is globally asymptotically stable. (d) shows the global stability of the pseudo-equilibrium E_P for $E_{I_b} < I^*_{b1}$ when $R_{01} > 1 > R_{012}$. Parameters values are $c = 8, \mu_m = 2, \mu_b = 0.8, \beta_{mb} = 0.3, \beta_{bm} = 0.18, f_m = 1, f_b = 0.4, \Lambda_m = 5, \Lambda_b = 2, E_{I_b} = 0.6$ such that $R_{01} = 2.16 > 1 > 0.96 = R_{02}$ and $E_{I_b} < I^*_{b1}$.

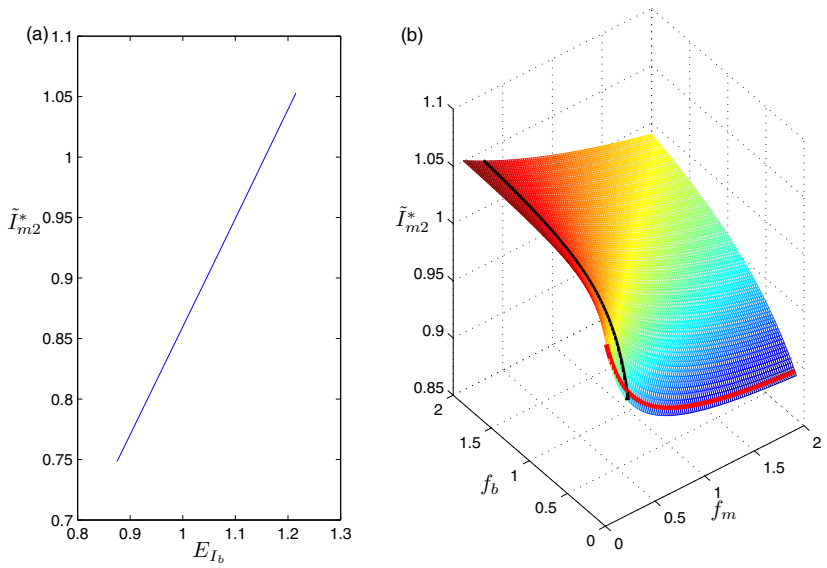

Fig 6: Plots of the value of $\tilde{I}^*_{m2}$ varies with E_{I_b} and f_m, f_b. (a) The value of $\tilde{I}^*_{m2}$ increases as E_{I_b} increases, with other parameters fixed as $c = 10, \mu_m = 2, \mu_b = 0.8, \beta_{mb} = 0.3, \beta_{bm} = 0.18, f_m = 0.3, f_b = 0.12, \Lambda_m = 5, \Lambda_b = 2$. (b) The mesh graph of $\tilde{I}^*_{m2}$ as a function of f_m and f_b and the intersecting curves with $f_m = 0.3$ (the black curve) and $f_b = 0.12$ (the red curve), respectively, with other parameters fixed as $c = 10, \mu_m = 2, \mu_b = 0.8, \beta_{mb} = 0.3, \beta_{bm} = 0.18, \Lambda_m = 5, \Lambda_b = 2, E_{I_b} = 1.1$.

stabilize at a previously chosen level E_{I_b}. Consequently, a combination of threshold control policy and the dynamics of the $free-system$ and $control-system$ brings a new equilibrium E_P at which the system (4) can stabilize under certain conditions, differing from the dynamic behaviour of system (9). This indicates that a previously chosen level of the desired number of infected birds can be reached by choosing proper combinations of threshold level and other parameters, which could provide a possible control strategy when an emergent infectious disease cannot be eradicated immediately.

Furthermore, when the new equilibrium E_P exists, if other parameters are fixed as in Fig 5, the value of the abscissa $\tilde{I}^*_{m2}$ of the new equilibrium is increasing as E_{I_b} increases, as shown in Fig 6(a). This implies that strict or frequent implementation of culling measure (corresponding to low threshold level E_{I_b}) will lead to the number of infected mosquitos decline. It follows from Fig 6(b) that increasing mosquito culling rate f_m decreases the equilibrium level of the infected mosquitos $\tilde{I}^*_{m2}$, while weakening bird culling rate results in a reduction of the infected mosquitos. It indicates that simultaneously culling both mosquitos and birds has different effect on equilibrium level of infected mosquitos. In particular, strengthening mosquito culling will be beneficial to curbing disease spread in mosquito population, which is associated with the conclusion by Xu et al.[22].

In this paper, we have established a model describing the non-instantaneous control of WNV transmission concerning a threshold policy for a WNV management and have qualitatively analyzed the dynamics of WNV transmission with culling control. The results show that the dynamics can be stable and useful from the viewpoint of WNV control, resulting in the number of infected birds remaining a previously given value. It is important to emphasis that the culling strategies in our model formulation are triggered when the number of infected birds is above a critical level. If given surveillance of mosquitoes, it may be more effective and economical to propose an additional threshold to trigger strategy of culling mosquitos, i.e., culling of mosquitoes is implemented only when the number of mosquitoes exceed a certain level, while culling of birds is also dependent on the density of infected birds. We leave this topic for further work. Note that this study is a bit disease specific, since the piece-wise smooth model is proposed to describe

WNV transmission dynamics, but we hope the approaches we used are able to be applied other vector-borne diseases such as Zika Virus [34] which was declared as a public health emergency of international concern (PHEIC) in 2016 [35]. This will fall within the scope of our future work by discussing the use of pesticides to cull mosquitoes as an effective strategy to prevent the spread of Zika Virus, owing to the absence of effective drug therapy against Zika Virus [36].

Acknowledgements

The authors were supported by the National Natural Science Foundation of China(NSFC, 11171268, 11571273(YX)), and by the Fundamental Research Funds for the Central Universities (08143042 (YX)), and by the International Development Research Center, Ottawa, Canada(104519-010).

References

[1] K.C. Smithburn, T.P. Hughes, A.W. Burke, J.H. Paul, A neurotropic virus isolated from the blood of a native of Uganda, Am. J. Trop. Med. Hyg. 20 (1940) 471-492.

[2] L.G. Campbell, A.A. Martin, R.S. Lanciotti, D.J. Gubler, West Nile Virus, Lancet Infect. Dis. 2 (2002) 519.

[3] N. Komar, S. Langevin, S. Hinten, et al, Experimental infection of North American birds with the New York 1999 strain of West Nile virus, Emerg. Infect. Dis. 9 (3) (2003) 311-322.

[4] C. Bowman, A.B. Gumel, P. Van den Driessche, A mathematical model for assessing control strategies against West Nile virus, Bull. Math. Biol. 67 (2005) 1107-1133.

[5] G. Cruz-Pacheco, L. Esteva, J.A. Montaño-Hirose, C. Vargas, Modelling the dynamics of West Nile virus, Bull. Math. Biol. 67 (2005) 1157-172.

[6] K.W. Blayneh, A.B. Gumel, S. Lenhart, T. Clayton, Backward bifurcation and optimal control in transmission dynamics of West Nile virus, Bull. Math. Biol. 72 (2010) 1006-1028.

[7] R.S. Lanciotti, J.T. Rohering, V. Deubel, et al, Origin of the West Nile Virus responsible for an outbreak of Encephalitis in the Northeastern United States. Science 286 (1999) 2333-2337.

[8] D. Nash, F. Mostashari, A. Fine, et al, The outbreak of West Nile virus infection in the New York City area in 1999, N. Engl. J. Med. 344 (2001) 1807-1814.

[9] http://www.cdc.gov/westnile/index.html.

[10] S.A. Gourley, R. Liu, J. Wu, Eradicting vector-borne diseases via age-structured culling, J. Math. Biol. 54 (2007) 309-335.

[11] J.M. Tchuenche, C.T. Bauch, Can culling to prevent monkeypox infection be counter-productive? Scenarios from a theoretical model, J. Biol. Syst. 20 (2012) 259-283.

[12] D.M. Thomas, B. Urena, A model describing the Evolution of West Nile-like Encephalitis in New York City, Math. Comput. Model. 34 (2001) 771-781.

[13] M.J. Wonham, T. de-Camino Beck, M.A. Lewis, An epidemiological model for West Nile virus: invasion analysis and control applications, Proc. R. Soc. London B 271 (2004) 501-507.

[14] M. Lewis, J. Renclawowicz, P. van den Driessche, Traveling waves and spread rates for a West Nile virus model, Bull. Math. Biol. 68 (2006) 3-23.

[15] V.M. Kenkre, R.R. Parmenter, I.D. Peixoto, L. Sadasiv, A theoretical framework for the analysis of the West Nile virus epidemic, Math. Comput. Model. 42 (2005) 313-324.

[16] J. Jiang, Z. Qiu, J. Wu, H. Zhu, Threshold conditions for West Nile virus outbreaks, Bull. Math. Biol. 71 (2009) 627-647.

[17] M. Lewis, J. Renclawowicz, P. van den Driessche, M. Wonham, A comparison of continuous and discrete-time West Nile virus models, Bull. Math. Biol. 68 (2006) 491-509.

[18] R. Ross, The Prevention of Malaria, second ed. Murray, London, 1911.

[19] G. Macdonald, The analysis of equilibrium in malaria, Trop. Dis. Bull. 49 (1952) 813-828.

[20] X. Hu, Y. Liu, J. Wu, Culling structured hosts to eradicate vector-borne diseases, Math. Biosci. Eng. 325 (2009) 496-516.

[21] R.R.L. Simons, S.A. Gourley, Extinction criteria in stage-structured population models with impulsive culling, SIAM J. Appl. Math. 66 (2006) 1853-1870.

[22] X. Xu, Y. Xiao, R.A. Cheke, Models of impulsive culling of mosquitoes to interrupt transmission of West Nile virus to birds, Appl. Math. Model. 39 (2015) 3549-3568.

[23] Y. Xiao, X. Xu, S. Tang, Sliding mode control of outbreaks of emerging infectious diseases, Bull. Math. Biol. 74 (2012) 2403-2422.

[24] Y.Xiao, T. Zhao, S. Tang, Dynamics of an infectious disease with media/ psychology induced non-smooth incidence, Math Biosci Eng. 10(2013) 445-461.

[25] T. Zhao, Y. Xiao, R.J. Smith?, Non-smooth plant disease models with economic threshold, Math. Biosci. 241 (2013) 34-48.

[26] A. Wang, Y. Xiao, A Filippov system describing media effects on the spread of infectious diseases, Nonlinear Anal.-Hybri. 11 (2014) 84-97.

[27] S. Tang, J. Liang, Y. Xiao, R A. Cheke, Sliding bifurcations of Filippov two stage pest control models with economic thresholds, SIAM J. Appl. Math. 72 (2012) 1061-1080.

[28] S. Tang, J. Liang, Global qualitative analysis of a non-smooth Gause predator-prey model with a refuge, Nonlinear Anal.-Theor. 76 (2013) 165-180.

[29] J. Yang, S. Tang, R A. Cheke, Modelling the regulatory system for diabetes mellitus with a threshold window, Commun. Nonliear Sci. 22 (2015) 478-491.

[30] L. Cherkas, Dulac functions for polynomial autonomous systems on a plane, Diff. eqs. 33 (1997) 692-701.

[31] A.F. Filippov, Differential Equations with Discontinuous Righthand Sides, Kluwer Academic, Dordrecht, 1988.

[32] V.I. Utkin, Sliding Modes in Control and Optimization, Springer, Berlin, 1992.

[33] S.M. Baer, B.W. Kooi, Y.A. Kuznetsov, H.R. Thieme, Multiparametric bifurcation analysis of a basic two-stage population model, SIAM J. Appl. Math. 66 (2006) 1339-1365.

[34] M.N. Balm, H. Lee, L. Chiu, E.S. Koay, J. Tang, A diagnostic polymerase chain reaction assay for Zika virus, J. Med. Virol. 84 (2012) 1501-1505.

[35] http://www.cdc.gov/zika/about/index.html.

[36] W.G. Brogdon, J.C. McAllister, Insecticide resistance and vector control, Emerg. Infect. Dis. 4 (1998) 605-613.